

# SYNTHESIS REPORT

## FOR PUBLICATION

CONTRACT N° : BRE 2-CT92-0147

PROJECT N° : BE 5099

TITLE : Method for making cm-size single crystal plates  
of diamond

PROJECT  
COORDINATOR : Prof.dr. L.J. Giling (KUN)

PARTNERS : Prof.dr. A. Gicquel (LIMHP)  
Mr. J.P. Dan (CSEM)

STARTING DATE : 01-01-1993

DURATION : 36 MONTHS



PROJECT FUNDED BY THE EUROPEAN  
COMMUNITY UNDER THE BRIT/EURAM  
PROGRAMME

DATE : 23-02-1996

# Method for making cm-size single-crystal plates of diamond: The “MOSAIC” process

*L.J. Giling, G. Janssen, J.J. Schermer,  
J.J.L. Spaanjaars, R.J.H. Klein-Douwel, J.J ter Meulen  
KUN : University of Nijmegen,  
Toernooiveld 1, 6525 ED Nijmegen, Netherlands*

*A. Gicquel, C. Findeling, E. Anger, K. Hassouni, A. Vignes  
LIMHP : Laboratoire d'Ingénierie des Matériaux et des Haute Pressions,  
Avenue J.B. Clément, 93430 Villetaneuse, France*

*H. Hintermann, J.P. Dan, W. Hänni, P. Alers, C. Faure  
CSEM : Centre Suisse d'Electronique et de Micro technique SA,  
Rue Jaquet-Droz 1, Case Postale 41, CH-2007 Neuchâtel, Switzerland*

## Abstract

A method, called the “MOSAIC”-process, has been developed for producing large-area, single-crystal, diamond plates. It starts by carefully orienting and closely packing a set of diamond seed crystals. This assembly, or mosaic, is then overgrown by chemical vapour deposition (CVD) with a single-crystal diamond layer. The success of the “MOSAIC”-process was shown for three different CVD techniques, namely the hot filament method (HF-CVD), microwave plasma assisted CVD (MPACVD) and the acetylene-oxygen combustion flame. The largest mosaic structure successfully overgrown -up to now- consists of seven semi crystals and has a surface area slightly in excess of 1 cm<sup>2</sup>. Although several technical problems still have to be solved, there seem to exist no fundamental reasons which could hamper the further enlargement of the surface area.

In order to realize the “MOSAIC”-process, know-how had to be developed about the diamond synthesis processes. Spatially resolved spectroscopic analyses provide information about the local characteristics of the growth environment. The MPACVD system was studied by optical emission spectroscopy (OES) and laser spectroscopy while the combustion flame was studied by laser induced fluorescence (LIF). The molecular density distributions of different species (H, C<sub>2</sub>, CH, C<sub>2</sub>H, OH) and their rotational temperatures (H, H<sub>2</sub>) have been determined. These results provide essential input data for the optimization and validation of modelling calculations, necessary to unravel the chemistry and dynamics of the dominant precursors, which in-turn are indispensable for the optimization and up-scaling of the deposition processes.

## 1. Introduction

Potentially, high quality diamond plates can form a new class of materials for the optical industry (windows, mirrors or lenses e.g. for high power lasers) and the electronic industry (substrates for diamond devices and/or radiation resistant components e.g. high energy radiation/particle detectors). However, in order to use diamond's unique properties [1] to its full potential it will be necessary to have a large and controlled supply of very high quality, single-crystal diamonds of sufficient dimensions. For example, to produce diamond-based electronic devices competitive to other wide band gap semiconductors it will be necessary to have at one's disposal diamond wafers

of at least one inch in diameter, while a single production unit would easily require 10,000 wafers/year. Even when using 1 cm<sup>2</sup> diamond plates the world-wide supply of suitable natural diamonds is short by several orders of magnitude. High pressure synthetic diamonds might be a temporary alternative, but the size of these diamonds will always be limited. Thus, if a high-tech diamond market is to emerge in the future, the necessary diamonds must be produced by CVD techniques.

A few years ago we therefore started to develop a process by which large-area, single-crystal diamond plates -suitable for optical and electronic purposes- can be made. The basic principle of this so called "MOSAIC" process is illustrated in figure 1 and can be described as follows. A number of natural (or high pressure synthetic) diamond seed crystals are carefully selected, polished, oriented and assembled in a closely packed arrangement (the mosaic) on a suitable substrate. Finally the mosaic is overgrown with a single-crystal diamond film using a CVD technique. Other approaches to obtain larger, nearly single-crystal, diamond plates from an array of seed crystals have been reported by Geis et al. [2] and later on by Posthill et al. [3, 4].

The present paper gives an overview of the results obtained in our laboratories using several variations of the "MOSAIC"-process, along with some of the related research necessary to achieve this. The progress made so far indicates that the "MOSAIC"-process might one day become the basis for a bulk diamond technology.

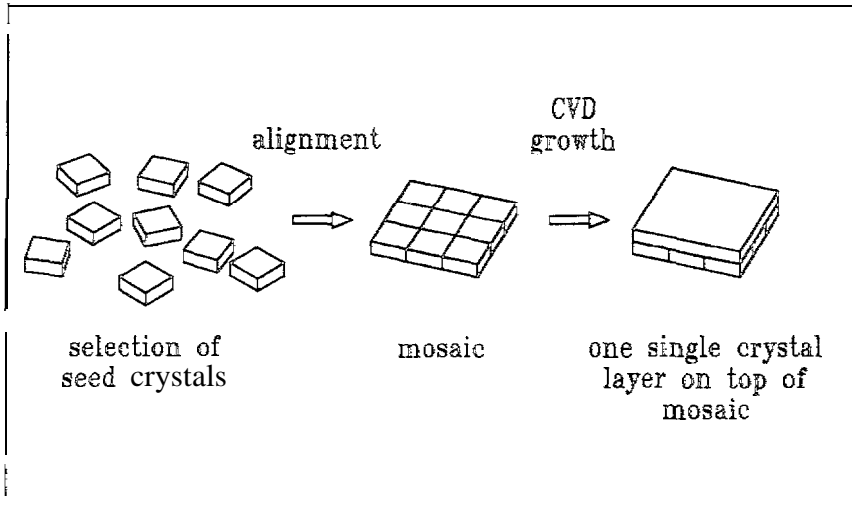


**Figure 1:** Basic principle of the "MOSAIC"-process.

## 2. Experimental

### 2.1 Diamond deposition systems

A priori, it was assumed that the successful overgrowth of mosaic structures might be dependent on the applied growth technique. Thus three, fundamentally different, deposition techniques were employed namely HF-CVD (at KUN), MPACVD (at LIMHP) and the flame (at KUN and CSEM). Each of the deposition techniques has its own characteristics and requirements which affect the diamond growth and the "MOSAIC"-process in particular.

HF-CVD: The conventional HF-CVD set-up optimized for homoepitaxial diamond growth has been described elsewhere [5]. Optimal conditions for growth on {001} faces are  $T_{fil} \approx 2500^\circ\text{C}$ ,  $T_{sub} = 650\text{-}900^\circ\text{C}$ , 1% CH<sub>4</sub> in H<sub>2</sub> at 50 mbar and 300 seem total flow. This gives growth rates of  $\approx 1 \mu\text{m/h}$ . Higher growth rates (up to 5  $\mu\text{m/h}$ ) are possible but generally yield lower quality

material. The filament lifetime (>250 hours) and the system stability have been increased well beyond the limits required for mosaic growth (10-50 hours). The deposition conditions used during HF-CVD were optimized for {001} growth. As these conditions are non-ideal for {111} growth, it will lead to extensive twinning and finally deterioration of the {111} faces when these facets develop during prolonged growth of the {001}.

**MPACVD:** The silica bell-jar MPACVD reactor with an independent y cooled or heated substrate holder was described elsewhere [6]. It was fed with methane (O - 5%) diluted in hydrogen and operated under moderate pressure conditions (20-80 mbar). Either a 1200 or a 6000 W microwave generator (2.45 GHz) was used for the activation of the gases. Optimal conditions for homoepitaxial diamond growth on {001} faces are  $T_{\text{sub}} = 780\text{-}850^{\circ}\text{C}$ , 1-4%  $\text{CH}_4$  in  $\text{H}_2$ , relatively high plasma power densities ( $P_{\text{MW}} = 15\text{-}23 \text{ W/cm}^3$ ) and 0-400 ppm  $\text{N}_2$ . Typically the growth rates range from 0.5 to 5  $\mu\text{m/h}$  and increases with increasing  $P_{\text{MW}}$ . The nitrogen is added to increase the growth rate and improve the morphology of the epitaxial layer.

**Combustion flame:** The basic set-up for flame growth used at the KUN was described elsewhere [7]. Using commercial burners and laminar flames the optimized conditions for high quality growth on {001} faces were  $T_{\text{sub}} \approx 1050^{\circ}\text{C}$ ,  $S_{\text{ac}} \approx 3\%$  at a distance flame front to substrate of 1.5 mm and a oxygen flow rate (in SLM) equal to  $1.4 \times d_0^2$  ( $d_0$  is diameter exit opening (in mm) of burner). This gives growth rates of 20-30  $\mu\text{m/h}$ . Higher growth rates (up to 100  $\mu\text{m/h}$ ) are possible, but result in a reduction of the quality and especially of the homogeneity of the deposit.

### 2.2 Initial investigate-m of homoepitaxial diamond deposition

Before the actual mosaic overgrowth, the growth of homoepitaxial diamond films by HF-CVD [8], MPACVD [9] and flame [10] was investigated in detail, For all three deposition set-ups diamond layers grown on {001} faces are superior in quality (lowest defect and impurity content) compared to all other directions of growth. However in order to fully employ the {001} growth it is necessary to obtain a more or less smooth surface without unwanted features like growth hillocks, random nuclei and penetration twins. This was achieved by (i) careful optimization of the deposition conditions and (ii) the growth on surfaces slightly disoriented from the exact {001} plane. In case of MPACVD the optimization was largel y supported by the spectroscopic investigations of the plasma (see also section 3.1). The disoriented faces provide a sufficient y high density of growth steps which suppress the formation of unwanted features. The optimal disorientation depends strongly on the deposition technique: 0-2° for the combustion flame, 2-4° for MPACVD and 4-7° for HF-CVD. All mosaics discussed below have {001} top faces (major growth plane) with a disorientation close to the optimal for the deposition technique used.

### 2.3 Characterization of diamond films

After growth the homoepitaxial diamond layers were routinely investigated by differential (Normarsky) interference contrast microscopy (DICM/NICM), scanning electron microscopy (SEM), Raman spectroscopy and cathodoluminescence (CL). Sometimes atomic force microscopy (AFM), X-ray diffraction, electron back scatter pattern (EBSP), infrared absorption spectroscopy or photoluminescence were included,

### 2.4 Mosaic assembling

The physical alignment of the seed crystals and the stability of the mosaic ensemble during CVD growth were considered of great importance. Several methods for assembling the mosaics were developed (KUN) and extensively tested for stability and compatibility with the growth of high quality homoepitaxial diamond (KUN, LIMHP).

### 2.4.1 Soldering techniques

High temperature soldering diamond to molybdenum has been described previously [11,12]. A tight-fitting recess is made in a molybdenum plate. This ensures the alignment of the seed crystals and prevents them from drifting away on the molten solder agent. Additional slits in the molybdenum are used to accommodate the excess solder. The recess-procedure is quite complicated, time-consuming (requiring six process steps) and very sensitive to errors. The final results in terms of alignment and separation ( $\leq 1 \mu\text{m}$ ) of the seed crystals can however be excellent [11]. As an alternative the mosaics can be soldered directly onto a flat molybdenum plate without the help of a recess. In this case the gap between the crystals is normally in the order of 10 to 50  $\mu\text{m}$  and the crystals have a tendency to rotate slightly relative to each other causing an additional misalignment [13].

In the case of flame deposition only these soldering techniques could be used because a good and stable thermal contact between the diamonds and the cooling device is absolutely essential for controlled growth during many hours [14]. The growth of diamond seems unaffected provided the solder is more or less stable in the flame. Somewhat surprisingly the large difference in thermal expansion between diamond and molybdenum does not induce significant stresses in diamond layers grown via the {001} “faces (i.e. no cracks, no shift of Raman LO-peak) even on repeated thermal cycling between room temperature and 1000- 1200°C [13].

The success of soldering in the flame growth is in sharp contrast with the results obtained for soldered diamonds in the HF-CVD and MPACVD systems. Here most of the solder agents are readily attacked by the strongly reducing atmosphere (atomic hydrogen and hydrocarbon radicals). This leads to a degrading of the solder contact or, even worse, to a complete deterioration of the homoepitaxial diamond growth. Such problems have been avoided successfully by careful processing during recess-soldering in order to minimize the contact between the solder agent and the aggressive atmosphere. Another problem is the use of molybdenum substrates. The large difference in thermal expansion between the diamond and the molybdenum often gives rise to stressed diamond films, leading ultimately to crack formation. This problem is strongly enhanced by the use of a tight-fitting recess as this considerably decreases the degree of freedom for stress relaxation [11],

### 2.4.2 Fluid fixation

In order to solve some of the problems with soldering techniques a much simpler assembling method, called fluid fixation, has been developed for HF-CVD and MPACVD. Fluid fixation [12] uses a thin film of a liquid to keep the diamonds (i) together and (ii) attached to a mirror-smooth silicon substrate. This liquid has a high surface tension, low vapour pressure and provides a good wetting of both diamond and silicon. The basic fixation procedure is similar to the one described by Geis et al. [2], but the use of about 100 times larger seed crystals in the “MOSAIC”-process makes the procedure much simpler. Depending on the accuracy of the lateral dimensions of the seed crystals and the skill of the operator the separation between the crystals can be as small as a few micrometers. Gaps between 10 and 20  $\mu\text{m}$  are easily attained. The fluid between the diamonds has a tendency to prevent them from drifting apart or turning relative to each other. After assembling a mosaic, it is immediately transferred to the reactor and the excess fluid is slowly evaporated by in-situ heating in a hydrogen atmosphere at reduced pressures. When handled with care, the quality (and morphology) of the diamond layers deposited immediately afterwards is not affected by the fluid. This is even true in case excess fluid was present on top of the diamonds. The silicon substrates are used because the difference in the thermal expansion between diamond and silicon for the interval between the deposition temperature (700-900°C) and room temperature is rather small. In general this was found to avoid the built up of thermal stresses and the formation of cracks.

## 2.5 “MOSAIC” *growth*

Diamond films have been deposited on top of several mosaic structures by HF-CVD, MPACVD or flame. Additionally a two-step procedure was developed in which a thick layer is grown by flame on top of an initial thin film deposited by HF-CVD or MPACVD. Based on the initial investigations discussed above, the seed crystals for the mosaics were chosen to be type IIa natural diamonds with {001} top faces, polished to the required orientations and dimensions by a commercial vendor. Unless stated otherwise the seed crystals were square diamond plates with dimensions of 2x2x(L5 mm<sup>3</sup>).

## 2.6 *Deposition area enlargement*

The present stage of the ‘MOSAIC’-process requires a reasonable homogeneous deposition area of several cm<sup>2</sup>. This is easily achieved for the HF-CVD and MPACVD set-ups. However, in case of the basic set-up (KUN) of the combustion flame, the deposition area is typically limited to 0.1-0.4 cm<sup>2</sup>. In order to increase this area, adaptations and optimisation of different types of burner nozzles were carried out (at CSEM). Especially interesting in this aspect were the modelling and experimental investigations of burner nozzles producing turbulent flames.

## 2.7 *Spectroscopic methods for analysing the diamond deposition systems*

Spatially resolved spectroscopic techniques were used to investigate the gas phase of the MPACVD system (at LIMHP) and the combustion flame (at KUN).

MPACVD: The microwave plasma of a similar set-up described in section 2.1 was analyzed by optical emission spectroscopy (OES) [15] and two photon allowed transition laser induced fluorescence (TALIF) [16].

Combustion flame: The flame of a similar set-up described in section 2.1 was analyzed by laser induced fluorescence (LIF) [17].

## 3. Results and discussion

### 3.1 *Spectroscopy of the MPACVD system*

By using laser diagnostics the gas temperatures and relative H-atom mole fractions were measured. Thereupon the relationships were established between these measurements, the temperatures of excited state species and the emission intensities ratio  $I_{\text{H}}/I_{\text{Ar}}$ . This made it possible to define “emission spectroscopic parameters”, measurable by OES, which are able to detect any evolution in the H<sub>2</sub> plasma system. These have been used then for controlling, optimizing and long-time in-situ monitoring the diamond deposition conditions by OES. The spatial distribution of the ground state and excited state H-atom temperature ( $T_{\text{H}}$ ) measured by TALIF were equal to the gas temperature ( $T_{\text{g}}$ ) [18]. Also the variation in  $T_{\text{H}}$  as a function of the plasma parameters (power density and percentage of methane) was investigated. From OES measurements of the radial distribution of the  $G^1\Sigma_g^+$  electronically excited state of molecular hydrogen, the rotational temperature  $T_{\text{R}}\text{H}_2(\text{G})$  was determined. To accomplish this an Abel inversion was performed of the line-of-sight OES measurements for each of the rotational lines of the  $G^1\Sigma_g^+ - B^1\Sigma_u^+(0,0)$  band. Their variations as a function of the power density are compared to those of  $T_{\text{H}}$ .

The variations of  $T_{\text{H}}$  (TALIF) were seen to be in very good agreement with the gas temperature calculated with the help of a 1-D diffusive model developed at LIMHP [19]. Diamond MPACVD reactors are characterized by very high temperatures. These temperatures are very sensitive to the averaged power density, and increase from 1550 K to 3100 K as the power increases from 6 to 30 W cm<sup>-3</sup>. The rotational temperature  $T_{\text{R}}\text{H}_2(\text{G})$  measured on the axis of the plasma is equal to approximately 3/4 of  $T_{\text{g}}$  and is not in equilibrium with the gas temperature even at pressures as

high as 20 to 50 mbar. This result disagrees with those of Cl-m et al [20], Owing to the very high efficiency of the quenching processes compared to that of thermalization,  $T_R H_2(G)$  should be equal to  $1/2 T_H H_2(X)$ . The proportionality factor  $3/4$  instead of  $1/2$  has been attributed to the G state excitation cross sections variations as a function of the rotational quantum number K, as suggested by Otorbaev [21] or to the variations of the radiative probabilities of the G state as a function of K. Although the Abel-inverted  $T_R H_2(G)$  is significantly lower than  $T_g$ , it follows the variations of  $T_g$  as a function of the operating conditions (see figure 2a) in particular the averaged microwave power density. Under the experimental conditions tested here, the G state rotational temperature has been proposed as an interesting “spectroscopic parameter”. Line-of-sight averaged  $T_R H_2(G)$  temperature, although lower by around 800 K than  $T_g$ , was also seen to follow  $T_g$  as a function of the power density. It can be used as well for monitoring the plasma conditions, in bell jar reactors.

The possibility was investigated to use the optical emission spectroscopy for measuring the relative concentration of the ground state H-atom. Two Photon Allowed transition Laser Induced Fluorescence and Optical Emission Spectroscopy have been used for (i) analyzing the variations of the H-atom mole fraction ( $x_H$ ) as a function of the operating conditions (percentage of methane in the feed gas and power density), and (ii) spatially (axially and radially) analyzing the plasma. The validity of the spectroscopic method of actinometry (measurement of  $I_H/I_{Ar}$  for estimating the evolution of  $x_H$ ) has been carefully analyzed (i) as a function of the operating conditions, (ii) for a spatial analysis of the plasma.

Actinometry can be used under conditions where the electron temperature is less than 20000 K and the H-atom mole fractions more than a few percent. In addition correcting factors must be taken into consideration. The correcting factors have been determined through a comparison of measurements from TALIF and OES or through calculations. In this way the quenching cross section of the excited 4p (2p1) argon state by molecular hydrogen was estimated to be  $42 \pm 30 \text{ \AA}$ . The quenching cross-sections of excited 4p (2p1) argon state and of excited H(n=3) state by atomic hydrogen have been estimated on basis of the hard sphere model or the energy Lennard-Jones potential curves found in the literature. Thus the TALIF measurements could be calibrated, which made it possible, for the first time, to determine the variations of the absolute H-atom mole fractions in microwave diamond deposition plasma reactors as a function of operating parameters. The calibration has been realized by comparing the experimental depletion of the H atoms observed as the methane is introduced in the discharge, at low H-atom mole fraction, to that calculated with a 0 dimension chemical kinetics model working in  $H_2 + CH_4$ . A H-atom mole fraction of 0.04 was found for an averaged power density of  $9 \text{ W cm}^{-3}$  ( $T_g = 2150 \text{ K}$ ). A decrease of the H-atom mole fraction is only observed under conditions where the H-atom mole fraction has the same magnitude as the methane percentage introduced in the feed gas. At high power density, no decrease is observed.

With these correction factors, it was found that the H-atom mole fraction increases from  $0.01 \pm 0.005$  to around  $0.32 \pm 0.15$  as the power density increases from  $6 \text{ W cm}^{-3}$  to  $30 \text{ W cm}^{-3}$  (see figure 2b). The experimental H-atom mole fraction is also seen to be in relative good agreement with that calculated with the 1-D diffusive  $H_2$  plasma (where energy and mass balance equations are solved and the surface reactions considered), owing to the large experimental error and to the approximations made for establishing the model. The dissociation mechanism of molecular hydrogen is mainly attributed, at low power density ( $6-12 \text{ W cm}^{-3}$ ), to the efficiency of the electron-molecule collisions ( $T_e$  high,  $T_g$  moderated), while, at high power density ( $>20 \text{ W cm}^{-3}$ ), it is attributed to the thermal processes efficiency ( $T_e$  is lower, and  $T_g$  higher).

Spatial distributions of  $I_H/I_{Ar}$ ,  $x_H$ ,  $T_H$  and  $T_R H_2(G)$  reveal strong radial non uniformities in these plasmas, and very high fluxes of species and energy at the diamond surface in growth. There are only two emissive carbon containing species (CH and  $C_2$ ) that have emission intensities suitable

for measurement by OES. Calculations showed that information on the plasma reactivity could be found by measuring the emission intensities ratio  $I_{C_2}/I_{Ar}$ , as well as  $I_{CH}/I_{C_2}$ . This last ratio provides information on the diamond quality as a function of the percentage of methane added (it is related to the variations of  $[CH_3]/[C_2H_2]$ ), while  $I_{C_2}/I_{Ar}$  gives information on the efficiency of the methane dissociation as the power density increases. The diamond growth rate was found not only to depend on the concentration of carbon containing radicals, but also an almost linear dependence of the growth rate on the H-atom mole fraction was observed. Using this knowledge, growth rates up to  $.5 \mu\text{m/h}$  could be reached, while maintaining a high quality of the epitaxial diamond layer. With this work, it was established at LIMHP that optimization of industrial MPACVD reactors by simultaneous measurements of the emission intensities ratios  $I_{Ha}/I_{Ar}$ ,  $I_{CH}/I_{C_2}$  and  $I_{C_2}/I_{Ar}$ , and of the  $H_2(G)$  temperature is possible. Furthermore, for long-term in-situ monitoring industrial reactors, the control of only the ratios  $I_{Ha}/I_{Ar}$  and  $I_{C_2}/I_{Ar}$  should be enough.

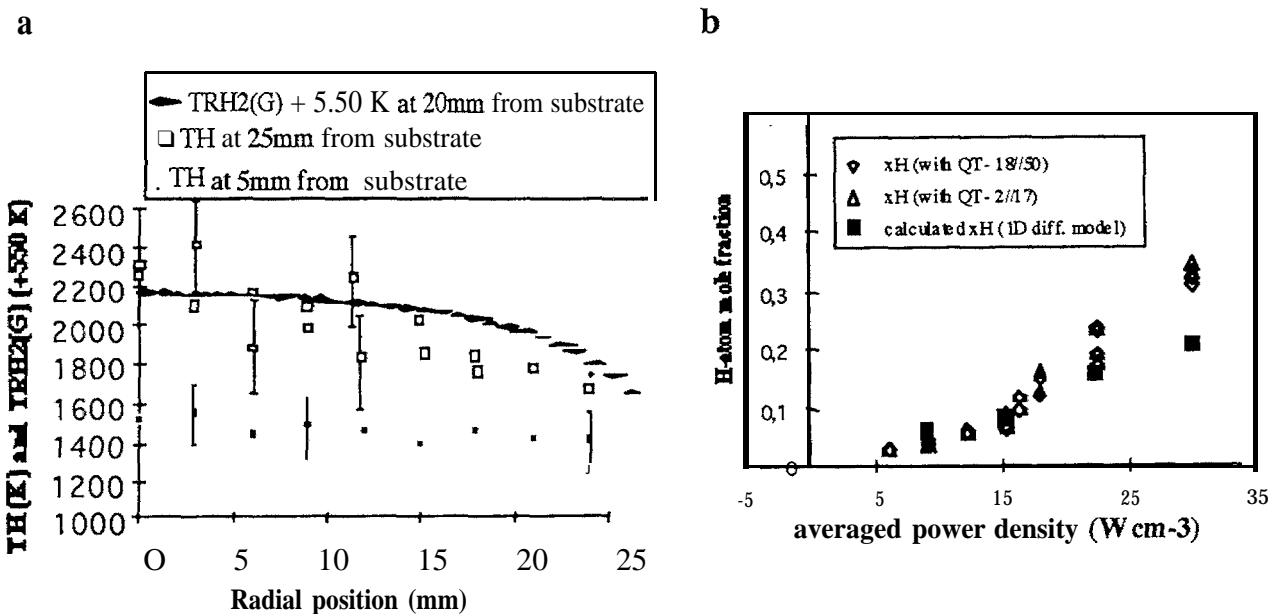


**Figure 2:** (a) Radial distribution of  $T_H$  (at 5 and 25 mm above the diamond substrate) and  $T_R H_2(G)$  (at 20 mm above the substrate) obtained for a plasma power density of  $9 \text{ W/cm}^3$ . (b)  $x_H$  as a function of the plasma power density obtained from the same measurements using two different sets of quenching cross sections. The values calculated from the I-D diffusive model are also given.

### 3.2 LIF of the combustion flame

LIF was used to determine 2-D, cross-section, mappings of the qualitative concentrations of OH, CH,  $C_2$  and  $C_2H$  in the combustion flame as a function of the deposition parameters. These results were correlated to the local growth rate and quality of the polycrystalline diamond films deposited simultaneously. In all experiments special attention is paid to the region of the boundary layer just above the substrate. The thickness of this boundary layer varies for each species and typically ranges from 100 to 600  $\mu\text{m}$ .

**OH:** Under diamond deposition conditions (reducing flame) OH is only present in the outer flame and not in the interesting zone just above the substrate. This implies a neutral (or negative) role for OH in diamond growth. In oxidizing flames OH is present in abundance.

**CH:** The CH concentration profiles show no clear relation to the diamond growth. However it is perhaps a good candidate for local temperature measurements using laser induced predissociative



fluorescence (LIPF). In this technique molecules are excited to a rapidly predissociating state which assures that the collected fluorescence signal is not disturbed by collisions. In normal LIF the large number of collisions in the atmospheric pressure flame prohibit a reliable measurement of the temperature. The CH molecule is a second choice for the LIPF technique, but the best candidate (OH) is not present in the flame. Unfortunately the signal to noise ratio is low in case of CH because of the narrow band spectral filtering necessary to suppress a broad band background fluorescence from large poly aromatic hydrocarbons (P-AH).

$C_2H$ : Despite intensive searches no detectable signals were observed from this molecule. Probably the  $C_2H$  concentration is much lower than predicted. Also more fundamental knowledge of spectroscopic parameters is necessary, in order to select the most favorable wavelength areas for excitation and detection.

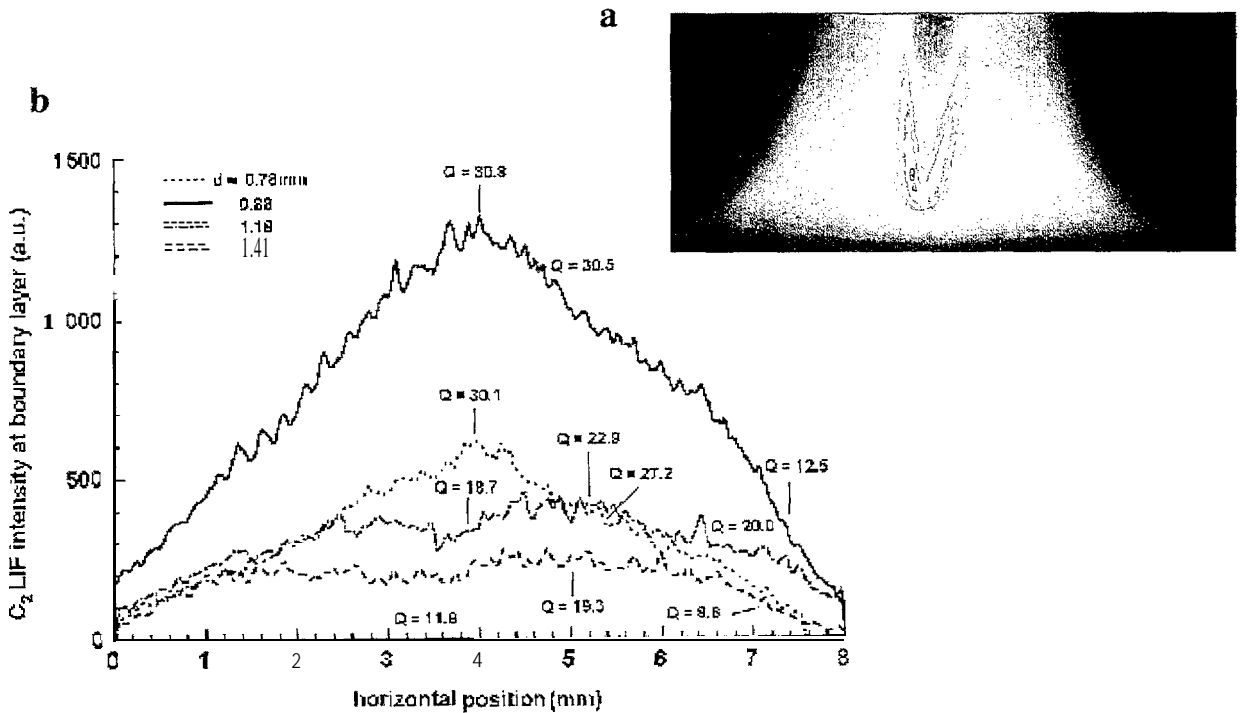


Figure 3: (a) Distribution of LIF signal of  $C_2$  measured at 438 nm (Swan band system). (b) Horizontal LIF intensity profiles of  $C_2$  just above the substrate for different distances  $d$ .  $Q$  is the quality factor of the diamond deposit as determined by Raman spectroscopy at the corresponding position at the substrate.

$C_2$ : This molecule is readily detected throughout the complete acetylene feather. Its LIF signal is maximal at the flame front and decreases sharply in a boundary layer just above the substrate (see figure 3a). The thickness and the horizontal structure of the  $C_2$  boundary layer' is dependent on the distance ( $d$ ) between the flame front and the substrate (see figure 3b) and the substrate temperature. A strong correlation was found between the  $C_2$  signal at the top of the boundary layer with the growth rate and the quality of' the deposited diamond film. These results have been described in more detail elsewhere [22].

### 3.3 Flame deposition area enlargement

On the base of an existing CSEM burner nozzle of 0.8 mm opening diameter creating a pure turbulent gas-stream (and therefore a turbulent flame) [23], a new generation of nuzzles has been developed. The development in steps from 0.8;1.4;1.7 to a final 2.2 mm diameter nozzle opening

has been fulfilled experimentally and optimised with the assistance of the model ANSYS/FLOWTRAN. A uniform, conformal, homogeneous and reproducible coating could be obtained on an area of up to 2 cm<sup>2</sup>.

With these nozzles it could be shown that the growth rate of homoepitaxial diamond layers was different for turbulent and laminar flames and that this effect depended on the direction of growth. On {111} faces the growth speed was identical for the laminar and turbulent flame deposition methods and was in the order of 25 μm/h for the given process condition. A small difference was found in the growth rate on {100} faces to the advantage of the turbulent flame giving a growth rate of 50 μm/h against 40 μm/h for the laminar flame. The most important growth rate difference between the turbulent flame and the laminar flame was observed on the {110} faces (200 μm/h relative to 100 μm/h, respectively). In general the coatings realised by the turbulent flames contained a smaller amount of amorphous carbon and residual graphite but a higher amount of nitrogen [24]. Later studies on comparing laminar and turbulent flames performed with the set-up at the KUN showed that the relative growth rates and deposition areas (in this case for polycrystalline, {111} and {001} growth) can easily interchange depending on the other deposition conditions [25].

For the deposition of diamond on surfaces from 2 to 5 cm<sup>2</sup> burners having an opening diameter of 2.7 to 3.4 mm had to be adapted. Purely turbulent flame burners of these dimensions are extremely dangerous when working with an acetylene/oxygen mixture. The flash back of the flame is so quick that it must be prevented with nitrogen. Therefore industrial burners working with a laminar gas flow operating close to the limit of turbulence have been considered for the follow up of the work. The very important heat formation of 30 to 50 kW by these big burners needed a new development of the substrate holder and its cooling system. With the modified substrate holder and a 3.0 mm opening nozzle a surface of 3 cm<sup>2</sup> could be uniformly coated with diamond.

Thus the original goal has been reached. The flame method is a very simple and readily available diamond coating process specially for thick film growth. But there are several inconveniences. Notably, there is an important consumption of the fluids, especially of acetylene which is expensive and not of the highest purity, and the incorporation of a non negligible amount of nitrogen in the diamond film coming from the impurities in the acetylene and the flame surrounding air. Strong corrosion is observed on the substrate holder due to the NO<sub>x</sub> containing exhaust gases. Nevertheless, the encouraging results of this development indicate ways to reach very high quality and thick diamond coatings for optical and electronic applications on substrates up to 20 cm<sup>2</sup> by replacing the flame method by a plasma torch method [26].

### 3.4 Growth on 'near-perfect' mosaics

In order to show the feasibility of the "MOSAIC"-process a trick was used to create mosaics in which the crystallographic alignment of the seed crystals relative to each other is almost perfect. To do this a larger diamond plate is laser-cut into several pieces, the cut faces are carefully polished and the original plate is reassembled using any of the techniques described in section 2.4. Such 'near-perfect' can have a crystallographic alignment well within 0.3°, while the height differences between the seed crystals are less than a few micrometers. Several 'near-perfect' mosaics, consisting of two, three or four seed crystals assembled by soldering or fluid fixation, have been overgrown by HF-CVD, MPACVD or the flame. Special attention was paid to the preferred orientation of the side faces of the seed crystals and the allowed width of the gap between the crystals.

HF-CVD: The first two mosaics both consisting of two seed crystals with {100} side faces, recessed to molybdenum (gap -1 μm) were successfully overgrown with one single-crystal diamond layer (14 respectively 40 μm thick) by HF-CVD. These mosaics have been extensively discussed previously [11,27]. Both mosaics contain {111} cracks (caused by the thermal mismatch

between diamond and molybdenum) which cross the joint region.

The overgrowth of a third, recess soldered, mosaic with {110} side faces and a wedge shaped gap (going from 1 to  $\approx 20 \mu\text{m}$ ) was less successful [12]. In order to bridge this larger gap, a relatively thick layer of about  $60 \mu\text{m}$  was deposited. However, before the initial gap was closed {111} facets had formed along the edges between the (001) top face and the {110} side faces. Such {111} facets have a strong tendency to form microtwins (parallel as well as inclined). After closing the gap this led to a bad morphology of the interface region showing a large number of penetration twins. On further growth the penetration twins increase in size at the expense of the top face. Apart from these features the quality of the film is good and the overgrown layer is probably one single crystal. After cessation of the growth also a {111} crack appeared along the original interface, obviously being the weakest spot.

Other experiments showed that high-quality, single-crystal overgrowth on mosaics with {110} side faces is possible. One such mosaics consisting of four seed crystals was assembled using fluid fixation (gap typically  $.5 \mu\text{m}$ ) in a stretcher-bond geometry which reduces the maximum number of joining faces from four to three [12]. No cracks appeared in the  $30\text{pm}$  thick epitaxial layer after growth.

An important feature on all HF-CVD grown mosaics, is that areas of enhanced growth occur parallel to the joints between the seed crystals. These regions have an appearance similar to a welding seam and are clearly propagating from the original joints but shifted by  $100\text{-}500 \mu\text{m}$  in the major step flow direction [11,12]. The enhanced growth is most probably caused by an enhanced growth step nucleation (compared to the normal {001} faces) due to the (misfit) dislocations occurring when two (or three) crystals of slightly different crystallographic orientations meet. Raman spectroscopy seems to support this idea. Excellent quality diamond is observed for parts of the layers deposited some distance away from the joining areas ( $\text{FWHM} = 2.8 \text{ cm}^{-1}$ ). Directly above the joints the FWHM increased slightly to  $3.0$  and  $3.7 \text{ cm}^{-1}$ , which is indicative of slightly defective material, e.g. due to dislocations. Sometimes the joint regions also show a shift of the peak position (plus or minus  $0.5 \text{ cm}^{-1}$ ) indicative of compressive and tensile stress, respectively. The shift of the enhanced growth relative to the original joints occurs because the dislocations propagate non-parallel to the normal growth direction. They are more or less 'pushed' in the direction of major step flow by the growth steps propagating across the surface. The distance of the shift is proportional to the thickness of the deposited film. In case of optimal HF-CVD conditions the shift is typically 5 to 10 times the thickness. When penetration twins are present in the joint region the enhanced growth area is pinned because the growth steps are hampered in crossing from one crystal to the other.

**MPACVD:** Similar experiments as described above were also performed by MPACVD. The results were however slightly different. First several mosaics consisting of two seed crystal with {100} side faces were overgrown. It was already found that in case of such side faces the (001) top face was expanding laterally, which is the preferred situation for "MOSAIC" growth. Indeed the overgrowth of these mosaics was easily proved to consist of one single-crystal diamond layer. As was the case for the mosaics overgrown by HF-CVD areas of enhanced growth occurred parallel to the joints. The enhancement is however less pronounced and the shift in the direction of the disorientation is relatively small, typically  $10 \mu\text{m}$  for a  $25 \mu\text{m}$  thick layer. Probably the disorientation from the exact {001} plane is no longer the dominating source of growth steps, but other sources generating random oriented steps have also become important. Therefore the 'pushing' behaviour of the steps does not have as distinct a direction as was the case in HF-CVD growth where these additional step sources seem to be less important.

In the case of seed crystals with {110} side faces it was observed that the (001) top face was shrinking due to the development of {111} facets along the edges of the crystals. As with the HF-CVD grown mosaics this easily led to the formation of penetration twins in the joint region,

especially when the width of the gap was too large and/or the physical alignment of the crystals was not good.

An important result obtained for MPACVD, was the possibility to suppress the undesirable penetration twins by the addition of some  $N_2$  (50 to 500 ppm) to the plasma. Furthermore it was possible to outgrow the penetration twins (formed in the diamond film during a previous deposition) by the deposition of a thick diamond layer in the presence of nitrogen (see figure 4). From these results it was concluded that nitrogen not so much prevents the formation of the twins, but rather changes the relative growth rates of  $\{111\}$  and  $\{001\}$  faces and thus the stability of the twin relative to the surrounding  $\{001\}$  face.

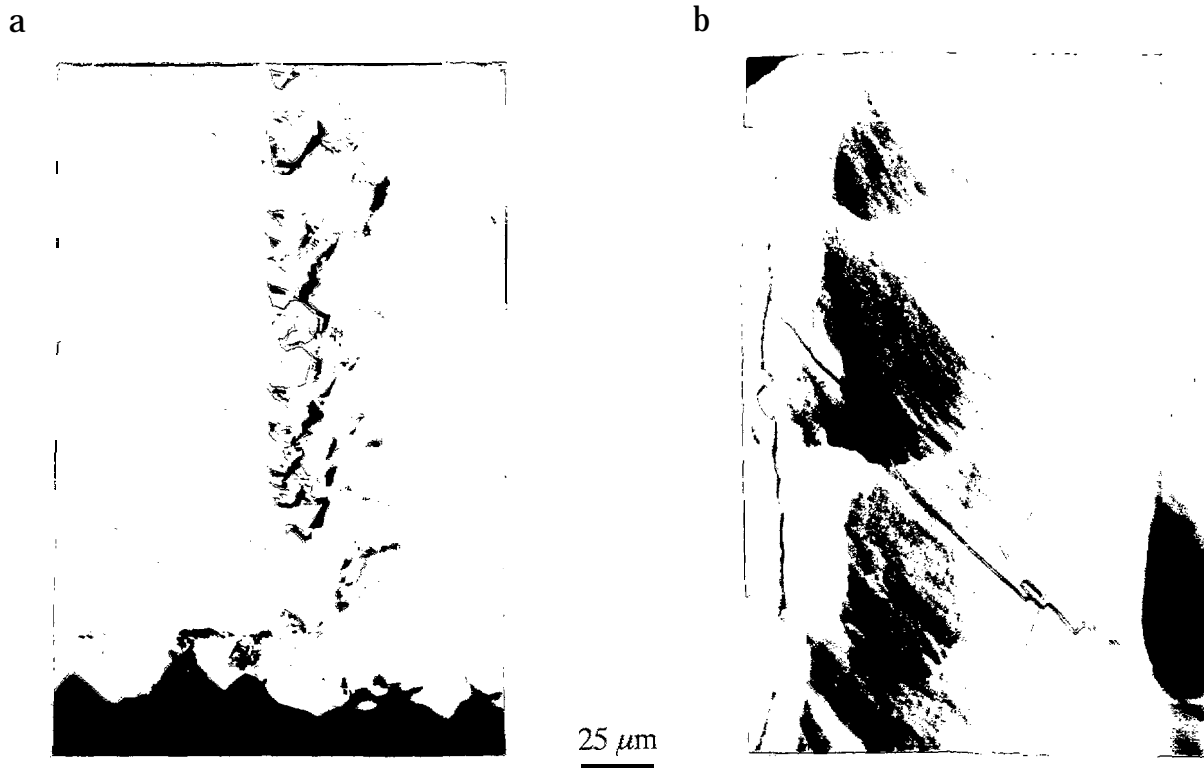


**Figure 4:** NICM images showing the joint region of a mosaic consisting of two seed crystal with  $\{100\}$  side faces overgrown by MPACVD. (a) After an initial film growth ( $25\ \mu\text{m}$ ) showing penetration twins and (b) after an additional layer ( $100\ \mu\text{m}$ ) grown in the presence of 100 ppm  $N_2$  (19 W/cm<sup>3</sup>, 1%  $CH_4$ , 800°C).

Thus the best quality layers were obtained at high power densities, i.e. high atomic hydrogen densities (see section 3.1), and with small quantities  $N_2$  present in the gas phase.

Combustion flame: It was found possible to grown  $\{001\}$  single crystals without imperfections at the rims by preceding the growth by an in-situ etching step in an oxygen rich flame [13]. Using this procedure it was possible to successfully overgrow several two piece mosaics. A particularly nice result was obtained for a mosaic consisting of three seed crystals directly soldered to molybdenum (see figure 5). Because of the triangular shape of the crystals both a  $[100]$  and a  $[110]$  gap was present. The widths of the wedge shaped gaps between the seed crystals varied from 7 to  $25\ \mu\text{m}$ . All three crystals were successfully overgrown with one single-crystal diamond layer as was easily demonstrated from the uninterrupted macrosteps and growth features above the original gaps. A more detailed description of this mosaic is given elsewhere [12,13].

Furthermore, the experiment demonstrated that the side faces at both sides of the gap not necessary need to be parallel. This and the relatively large gap width that could be bridged is of great importance because it allows small in-plane rotations of the individual mosaic substrates of which the side faces never have exactly the same crystallographic orientation. The fact that both the gaps along  $\langle 100 \rangle$  and along  $\langle 110 \rangle$  can be overgrown indicated that most probably gaps along any direction can be overgrown. So a large variety of substrate shapes might be used to be arranged in a mosaic structure. Micro-Raman analyses of the overgrown mosaics indicated that the increased dislocation density of  $\langle 110 \rangle$  joint regions might allow relaxation of strain at the joint. Nevertheless, a joint along  $\langle 110 \rangle$  is less favourable because this direction is parallel to the  $\{111\}$  cracking plane of diamond and involves the risk of fracturing the overgrown layer along the joint. Furthermore the development of defective  $\{111\}$  facets in these  $\langle 110 \rangle$  gaps can obstruct the formation of one single crystalline diamond layer on top of the mosaic structure.

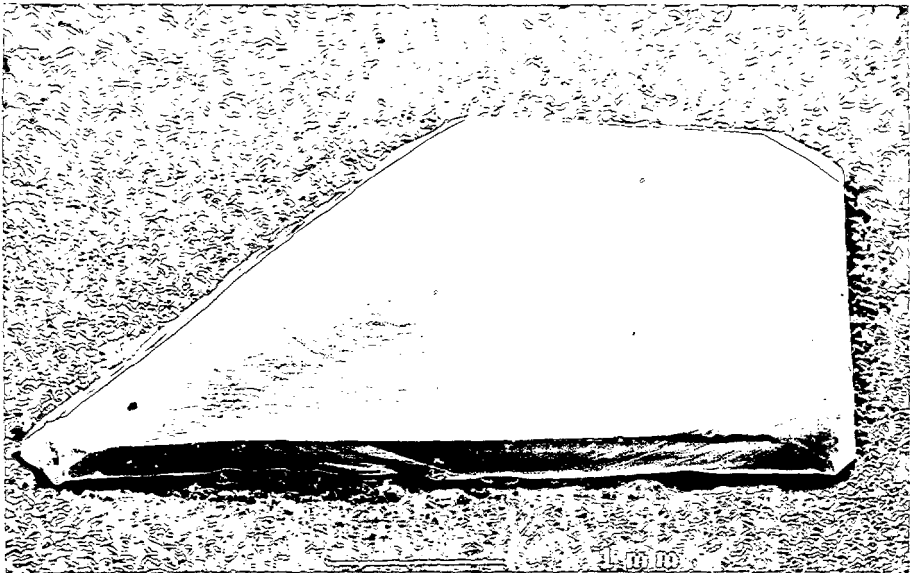


**Figure 5:** SEM image of mosaic consisting of three (001) right-angled triangular seed crystals (each with two sides of 2.25 mm) directly soldered to molybdenum after flame growth ( $S_{ac}=4-5\%$ ,  $T_{dep}\approx 1030^{\circ}\text{C}$ ,  $t=11$  hours,  $d\approx 250\ \mu\text{m}$ ), details are given in [13].

The main conclusion from these 'near-perfect' mosaics is that for all three deposition techniques the "MOSAIC"-process works, i.e. a **single-crystal overgrowth** can be obtained on closely packed and well aligned, seed crystals. The side faces can be either  $\{100\}$  or  $\{110\}$ . The direction of misorientation, and thus the major step flow direction, can be either perpendicular or parallel to the joint between the seed crystals.

### 3.5 "MOSAIC" growth by a two-step procedure

As an alternative to the direct overgrowth by a single deposition technique also a two-step procedure was developed which combines the merits of two techniques. The 'gentle' HF-CVD or MPACVD techniques are used to bridge the gap between the seed crystals and produce an initial, single-crystal overgrowth of  $\sim 20\ \mu\text{m}$  in thickness. Then the combustion flame, with its high growth rate, is applied to enlarge this crystal to a thickness larger than  $250\ \mu\text{m}$ . Of course this procedure puts additional requirements on the mosaic structure and its processing, but it also opens the possibility to use the easier fluid fixation in the first stages of the mosaic assembling. After coverage with a thin layer the mosaic structure can be handled more easily to allow direct

soldering to molybdenum without the problems of keeping the seed crystals closely packed and aligned. Especially for mosaics consisting of more than three seed crystals this is a definite advantage.

The two-step procedure was first tested for soldered mosaics. These are easily transferred to the flame. Some problems exist with the aging of the solder after prolonged growth by HF-CVD (typically 20 to 50 hours) and the additional thermal cycling (up to  $\sim 1300^{\circ}\text{C}$ ) in the final preparation for flame growth. Sometimes this results in a (partial) loss of thermal, or even physical, contact between the diamonds and the molybdenum. Compared to direct-soldered mosaics, the recess-soldered samples show a significantly better stability. Two 'near-perfect' mosaics with one single-crystal initial film grown by HF-CVD (see section 3.4) were transferred to the flame. After a short ( $\approx 1$  rein) etch period, a thick diamond layer exceeding  $250\ \mu\text{m}$  was deposited. Both layers remained single-crystal at the joint. These films are discussed extensively elsewhere [12,13,28].

Next a HF-CVD pre-grown mosaic with clusters of large penetration twins along the joint between the seed crystals was overgrown by flame in an attempt to remove or outgrow these undesirable features. It proved very difficult to remove the penetration twins, once they have been formed. Even after prolonged ( $>30$  rein) etching in the flame, some parts of the twins usually remain present. During subsequential growth the twins redevelop and often slowly increase in size at the expense of the epitaxial (001) top face of the film [12].

In case of mosaic structures obtained by the fluid fixation the transfer is more complicated. After dissolving the silicon substrate, the back side of the seed crystals have to be cleaned thoroughly and small polycrystalline diamond particles attached to the seed crystals have to be broken off by tweezers. Although mosaics with an overgrowth as thin as  $20\text{pm}$  can be handled, the removal of the polycrystalline film is a delicate job. Normally a thin fringe of in-grown crystallite remains attached. After cleaning the mosaic it is soldered to a molybdenum plate and transferred to the flame. Problems with the solder stability as described above are avoided, but the additional handling carries a risk of damage to the mosaic.

As an alternative it was also attempted to solder the mosaic structure up-side-down, i.e. with the grown layer attached to the molybdenum. After soldering this requires additional steps to remove (i) undesirable, but chemically stable, surface contaminations (silicon carbide) and (ii) the polycrystals embedded along the rims of the seed crystals. Classical diamond polishing has been used more or less successfully here, but diamond etching in the flame set-up provides a good and easy alternative [12,13]. Combined with the direct overgrowth by the combustion flame on such a well aligned mosaic, this provides a good route for processing of pre-grown mosaics with penetration twins and foreign particles at the interfaces.

### 3.6 Growth on 'true' mosaics

After the success of the small 'near-perfect' mosaics the investigations were first directed towards the limiting factors for successful overgrowth and next towards larger mosaics. The maximum allowable mismatch in the crystallographic alignment of the seed crystals relative to each other was tested by preparing intentionally misaligned mosaics. These mosaics, consisting of two seed crystals with in-plane misorientations between  $1$  and  $11^{\circ}$ , were overgrown by HF-CVD or the flame. Although a connected layer was obtained and the seed crystals were physically attached in all cases, the overgrowth was not a single-crystal. Careful inspection of the joints showed that even for the smaller misorientations a low angle grain boundary is present which often induces twin-like defects and polycrystalline inclusions. Only in case of a  $1^{\circ}$  disoriented mosaic some small portions of the joint form a connected single-crystal overgrowth.

In conclusion: single-crystal overgrowth is possible provided that the seed crystals are very well aligned (probably  $\leq 1^{\circ}$  mismatch in three directions), However, when starting from seed crystals

individually, oriented (using X-ray analysis), cut and polished from small diamonds it will be rather difficult to fulfil this requirement. The type IIa natural diamonds used here are mostly plastically y deformed and contain high densities of dislocations and slip bands [1]. These features give a so-called mosaic-spread on the crystallographic orientation which is readily observed as very broad spots/lines in X-ray diffraction. Thus it seems unrealistic to expect a total crystallographic alignment (in three directions) within a mosaic assembly to be better than within  $\pm 0.5^\circ$ , more probably  $\pm 1^\circ$ .

Based on these results and those described in sections 3.4 and 3.5 an optimal mosaic  $>1\text{ cm}^2$  for the HF-CVD system was designed. It consists of 7 seed crystals with a (001) top face disoriented  $5^\circ$  towards [110] and {100} side faces. Each crystal is  $4\times 4\times 0.5\text{ mm}^3$  in dimension which gives a total surface area of  $1.12\text{ cm}^2$ . In order to make this mosaic a fairly large natural diamond was sawn into several parallel plates. From these irregular shaped plates the seven seed crystals were cut and polished by the vendor to the required dimensions and orientations (within  $1^\circ$  relative to each other). Thus this mosaic consists of sufficiently well aligned, but more or less independently obtained, seed crystals. After fluid fixation the resulting mosaic was overgrown by HF-CVD with a  $25\text{ }\mu\text{m}$  thick diamond layer (see figure 2).

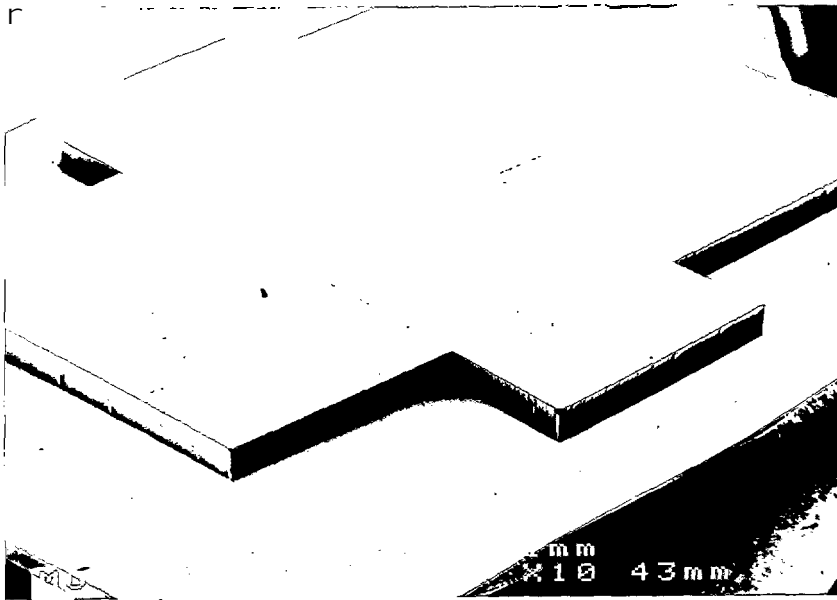


Figure 6: SEM image of single-crystal diamond film ( $25\text{ }\mu\text{m}$ ) of  $1.12\text{ cm}^2$  grown on top. of a mosaic consisting of seven (001) natural diamond plates each  $4\times 4\times 0.5\text{ mm}^3$  in dimension.

As before the seed crystals can be easily recognized from the areas of enhanced growth along the joints. More detailed investigations of the joint regions, 12 on the top face and 6 on the side faces with a total length of 35 mm, showed different types of morphologies. Some joints are completely dominated by large growth hillocks, which are sometimes correlated to penetration twins. Other joints show only very few hillocks and twins, while still others show no such features at all even on the side faces. The penetration twins along the interfaces are probably caused by sub-micron chip-out which was observed before deposition, along most of the edges between top and side faces. Along the exterior edges the chip-out develops into 'cusps' [7, 11]. From careful observations of the growth features on the crystals, as well as the occurrence of some {111} cracks crossing the interfaces, it was concluded that (apart from the penetration twins) six of the seven seed crystals have been successfully overgrown by one single-crystal diamond layer. The seventh crystal (most right in figure 2) is physically joined to the others but further investigations are required to determine whether the layer is single-crystalline at the joint.

#### 4. Conclusions

The combined efforts of the three partners involved in this project, i.e. KUN, LIMHP and CSEM, have led to the realization of the final goal of this project: a single crystal diamond layer in excess of  $1 \text{ cm}^2$ . The method which has been used to achieve this goal, the so-called "MOSAIC"-process, in principal is a surface enlargement process. So far no limitations have been observed for the enlargement process itself, so that even larger diamond crystal plates are possible by a repetition of the method. For the growth process all three available methods i.e. HF-CVD, MPACVD and the combustion flame can be used. At the present stage of knowledge, there is a slight preference for a two step procedure: at first the growth of a thin layer by either the hot-filament or plasma deposition process, followed by the growth of a thick layer by the flame method. However, it has been demonstrated that a one step process is also possible by using just the flame deposition method. 'This would further simplify the present "MOSAIC"-process. The quality of the produced diamond is good to excellent, depending on the growth conditions. The quality of the best single crystals, as judged by cathodoluminescence, Raman spectroscopy, infrared transmission spectroscopy and X-ray analyses, equals that of the best quality natural diamonds (type IIa).

The spectroscopic analysis of the plasma ball, which has been performed to unravel the processes in the plasma during diamond deposition, has been very successful. The analysis has revealed that the quality of the grown diamond is directly related to the absolute concentration of H-atoms and to the  $\text{CH}_3/\text{C}_2$  concentration ratio, The absolute concentrations of  $\text{CH}_3$  and  $\text{C}_2\text{H}_2$  are directly related to the growth rate. At higher power levels, also the H-atom concentration increases, what gives rise to a high quality of the grown diamond. Simultaneously the methane concentration can be raised without a loss of quality, resulting in an increased growth rate. A further result of the spectroscopic analysis has been, that direct possibilities exist to control the behaviour of the plasma ball by monitoring the intensities of the emissions of the  $\text{H}(\alpha)$  and  $\text{C}_2$  line with respect to the intensity of the Argon tracer emission.

The supporting diagnostics for the optimization of the flame, using LIF, has also given important information. A one to one correspondence has been found between the concentration profiles of CH and  $\text{C}_2$  and the growth rate of the diamond layer. At higher  $\text{C}_2$  concentrations the quality of the grown material appears to be improved. This has been correlated with the optimal distance between the tip of the flame and the growing surface.

The supporting research for the up-scaling of the oxy-acetylene burner, has shown that laminar flames operating at the onset of turbulence, are best suited for an up-scaling between 2 and  $3 \text{ cm}^2$  deposition area. Difficulties will arise with heat and noise production, corrosion and safety when still larger areas are wanted. Nevertheless, the encouraging results of this research have indicated that still larger areas are possible by using deposition by means of a plasma torch.

#### 5. Acknowledgements

The KUN and LIMHP part of this work was financially supported by the European Community through the Brite Euram 11 program as project BE 5099 under contract no BE2-CT92-0147. The CSEM part of the project was financially supported by the Swiss government under contract no OFES 92.0061 (BR230).

The KUN-group acknowledges the scientific and technical support of W.J.P. van Enckevort, P. Schmidt, G.Z. Cao, J. te Nijenhuis, W. Elst, F. de Theije, J. Soffner and P. Smits.

The LIMHP group wishes to thank M. Chenevier from Laboratoire de Spectrométrie Physique at Grenoble for the TALIF measurements and Y. Breton for assistance with the OES measurements.



## 6. References

- [1] J.E. Field (cd.), "The properties of natural and synthetic diamond", Academic Press, London 1992.
- [2] M.W. Geis, N.N. Efremov, R. Susalka, J.C. Twichell, K.A. Snail, C. Spiro, B. Sweeting and S. Holly, *Diamond Relat. Mater.* 4, (1994) 76.
- [3] D.P. Malta, J.B. Posthill, G.C. Hudson, R.E. Thomas, T.P. Humphreys, R.A. Rudder and R.J. Markunas, in "Proceedings of the fourth international Symposium on Diamond Materials", edited by K.V. Ravi and J.P. Dismukes (Electrochem. Soc. Proc. 95-4, Bennington, NJ 1995) 509.
- [4] J.B. Posthill, D.P. Malta, G.C. Hudson, R.E. Thomas, T.P. Humphreys, R.C. Hendry, R.A. Rudder and R.J. Markunas, *Thin Solid Films*, in press.
- [5] G. Janssen, "Homoepitaxial Diamond Synthesized by CVD Processes", Thesis, University of Nijmegen, (1994).
- [6] A. Gicquel, K. Hassouni, S. Farhat and Y. Breton, C. D. Scott, M. Lefebvre M. Pealat, *Diamond and Related Materials*, 3 (1994) 581.
- [7] J.J. Schermer, J.E.M. Hogenkamp, G.C.J. Otter, G. Janssen, W.J.P. van Enckevort and L.J. Giling, *Diamond Relat. Mat.*, 2, (1993) 1149.
- [8] G. Janssen, W.J.P. van Enckevort, W. Vollenberg and L.J. Giling, *J. Crystal Growth* 148 (1995) 355, and W.J.P. van Enckevort, G. Janssen, W. Vollenberg and L.J. Giling, *J. Crystal Growth* 148 (1995) 365.
- [9] C. Findeling-Dufour, A. Vignes and A. Gicquel, *Diamond Relat. Mat.*, 4, (1995) 429.
- [10] J.J. Schermer, W.J.P. van Enckevort and L.J. Giling, *J. Cryst. Growth* 148 (1995) 248.
- [11] G. Janssen and L.J. Giling, *Diamond Relat. Mat.* 4, (1995) 1025.
- [12] G. Janssen, J.J. Schermer and L.J. Giling, *Mater. Res. Soc. Proc.* 416 (1996) in press.
- [13] J.J. Schermer, F.K. de Theije and L.J. Giling, *J. Cryst. Growth*, (1996) in press.
- [14] J.J. Schermer, W.J.P. van Enckevort and L.J. Giling, *Diamond Relat. Mat.*, 3, (1994) 408.
- [15] A. Gicquel, M. Chenevier and M. Lefebvre, in "Handbook for Diamonds and Diamond films" eds. M. Prelas, G. Popovicci and K. Bigelow, section 7.2 "Modeling and diagnostics in plasmas", to be published (1996).
- [16] A. Gicquel, M. Chenevier, Y. Breton, M. Petiau, J.P. Booth and K. Hassouni, *J. de Physique III*, to be published (1996).
- [17] P. Andresen, A. Bath, W. Gröger, H.W. Lülff, G. Meijer and J.J. ter Meulen, *Appl. Optics* 27 (1988) 365.
- [18] A. Gicquel, M. Chenevier, K. Hassouni, J.C. Cubertafon, Y. Breton and A. Tserepi, *Diamond Relat. Mat.* 5 (1996), in press.
- [19] K. Hassouni, S. Farhat, C. Scott and A. Gicquel, *J. de Physique III*, to be published (1996).
- [20] H. N. Chu, E.A. Den Hartog, A. R. Lefkow, J. Jacobs, L. W. Anderson, M. G. Legally, J. E. Lawler, *Phys. Rev. A*, 44 (1991).
- [21] D. K. Otorbaev, V. N. Ochkin, P. L. Rubin, S. Yu Savinov, N. N. Sobolev, S.N. Tskhai, Technical report of the Lebedev Physics Institute, Academy of Sciences of the USSR, series editor N. G. Basov, vol. 179, supplemental volume, edited by Sobolev, translated by Kevin S. Hendzel, Nova Science Publishers, Commack, pp 121-173 (1989).
- [22] R.J.H. Klein-Douwel, J.J.L. Spaanjaars and J.J. ter Meulen, *J. Appl. Phys.* 78 (1995) 2086.
- [23] P. Alers, W. Hänni and H.E. Hintermann, *Diamond Relat. Mat.* 2 (1993) 393.
- [24] J.J. Schermer, P. Alers and L.J. Giling, *J. Appl. Phys.* 78 (1995) 2376.
- [25] J.J. Schermer, W. A.L.M. Elst and L.J. Giling, *Diamond Relat. Mat.* 4 (1995) 1113.
- [26] Work in progress at CSEM, to be published.
- [27] G. Janssen and L.J. Giling, in S. Saka et al. "Advances in New Diamond Science and Technology", MYU, Tokyo (1994) 295.
- [28] J.J. Schermer and L.J. Giling, in "Proceedings of the fourth international Symposium on Diamond Materials", edited by K.V. Ravi and J.P. Dismukes (Electrochem. Soc. Proc. 95-4, Pennington, NJ 1995).